

Optimal shift of pattern shifting for mitigation of mask defects in extreme ultraviolet lithography

Sikun Li, Xiangzhao Wang, Xiaolei Liu, Heng Zhang

Laboratory of Information Optics and Opto-Electronic Technology, Shanghai Institute of Optics and Fine Mechanics,
Chinese Academy of Sciences, Shanghai 201800, China.



INTRODUCTION

Mask defects, especially multilayer defects, are a major roadblock to EUV lithography adoption in high volume manufacturing. Although the defect density and size are reduced annually, the current progress is far from sufficient.

The defects in the blank are difficult to repair without damaging the blank itself. Therefore, the mitigation of mask blank defects is considered a well working alternative proposition. Several mitigation methods, such as mask floor planning, pattern shifting^{1,2} and absorber modification³, have been proposed. There is no reliable method which can repair all EUV blank defects. For better defect mitigation, several combination methods are proposed. Elayat et al.⁴ provided a cost-benefit assessment of different defect mitigation methods. It is demonstrated that the most promising methods are pattern shifting and its combination with other methods.

The optimal shift of pattern shifting needs to be determined when combined with other mitigation methods. Two methods for determining the optimal shift are presented in this study. The first method involves the mitigation of the impact of all defects as much as possible. For this method, a merit function is proposed to determine the optimal shift in pattern shifting. The second method attempts to cover as many defects as possible. A merit function is also proposed. These two methods are then compared.

MODELING ASSUMPTIONS AND PARAMETERS

First, the blank defects considered in the following are multilayer defects after smoothing deposition process. We assume that the blank defects are all Gaussian defects. Furthermore, we assume that the inspection tool provides the exact locations and sizes of the defects. The size of the defect is described by height and full width at half maximum (FWHM). In the simulation, the locations and sizes of defects in the blank are generated by adopting uniform random number.

In addition, all sizes reported here are at mask scale, and magnification is 4×. The mask layout consists of patterns of square reflective regions. According to the application of EUV lithography, the pattern size in the simulations is 64 nm, and pitch is 400 nm.

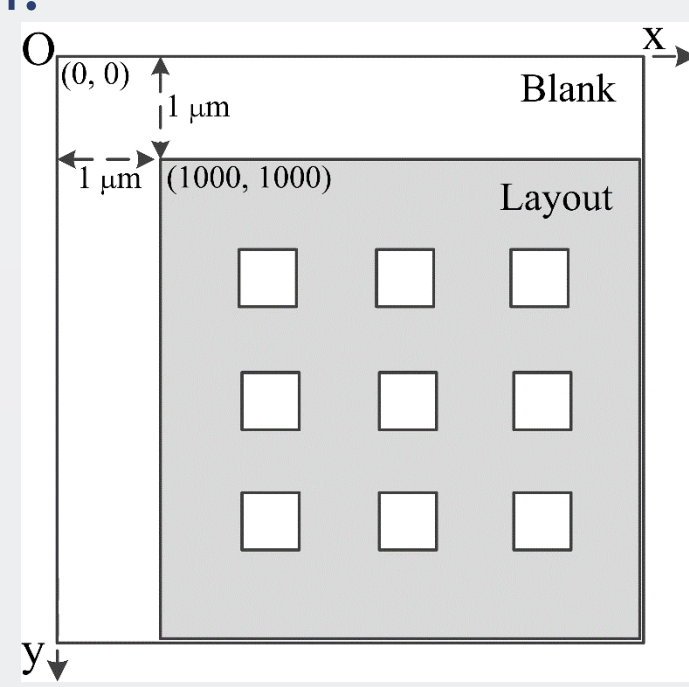


Fig. 1 Schematic of the mask blank, layout and margin

Considering the accuracy of the mask writer, 10 nm errors are included in the simulation. Normally, because the blank is always a little larger than the layout, a certain margin is kept between the layout and blank boundaries, allowing to shift the layout relative to the blank(Fig. 1). A layout without shifting means that the layout is positioned at the center of the blank. In our approach, the sizes of the layout and the blank are limited to 40 μm×40 μm and 41 μm×41 μm, respectively.

MINIMUM IMPACT METHOD

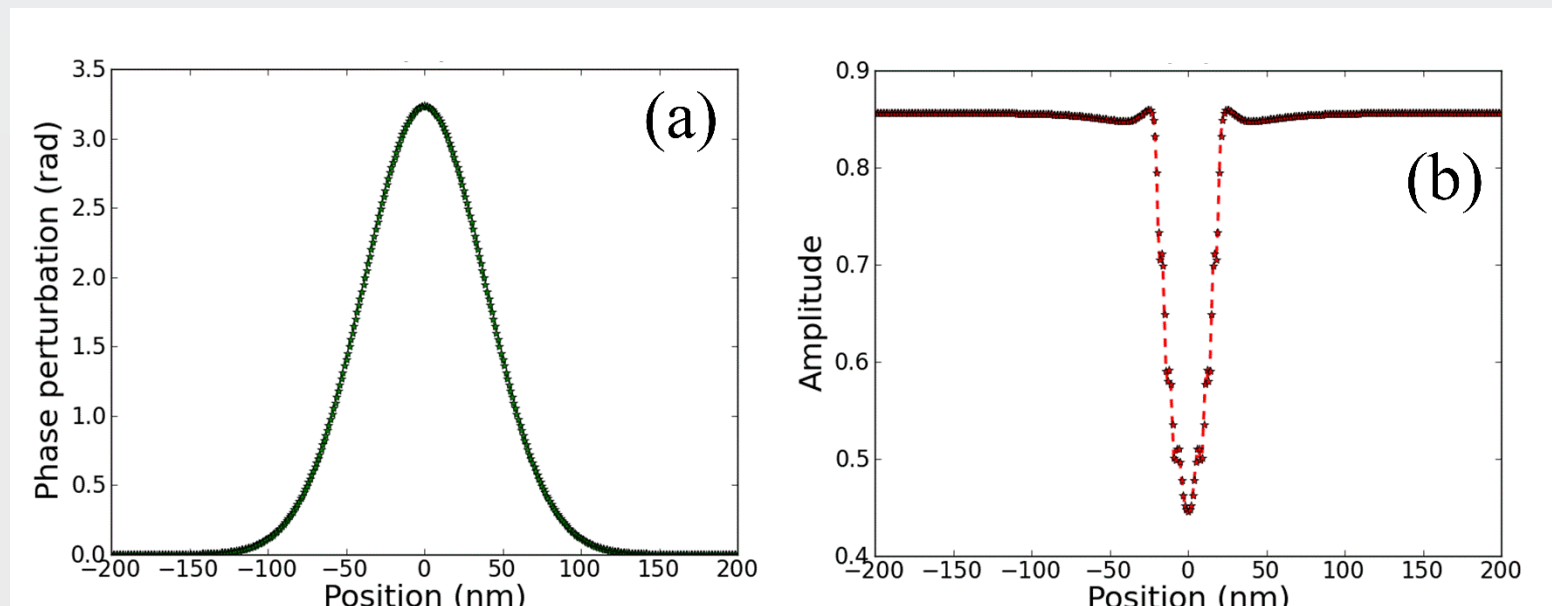


Fig. 2 The phase perturbation (a) and change of amplitude (b) of the multilayer reflection coefficient caused by a multilayer defect.

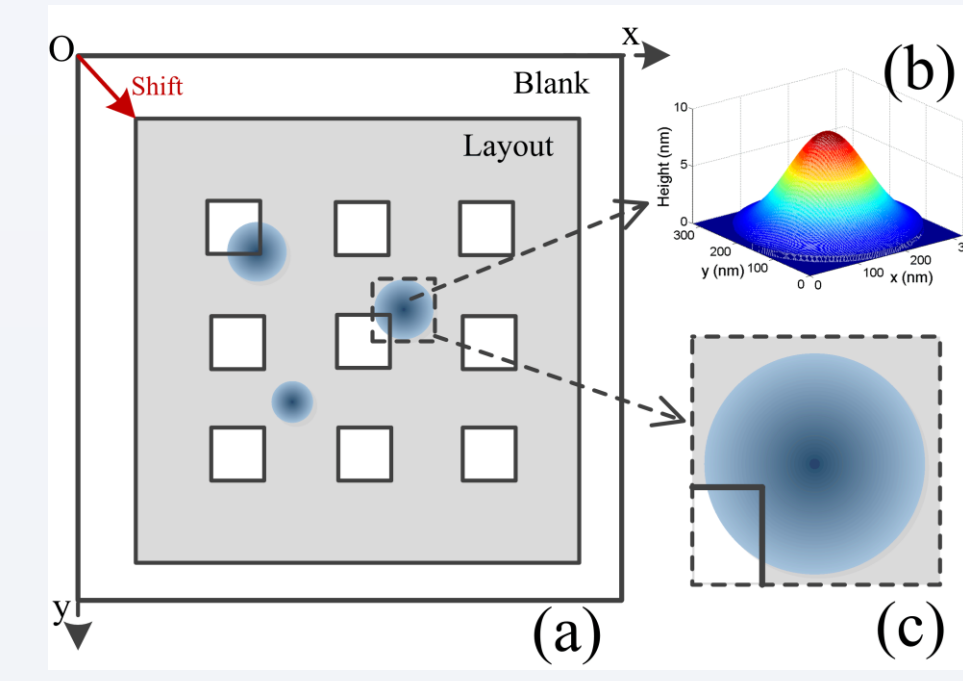


Fig. 3 (a) The relative position of the blank and layout after shifting, (b) the three-dimensional topography of the defect, and (c) the effective region for computation of the impact.

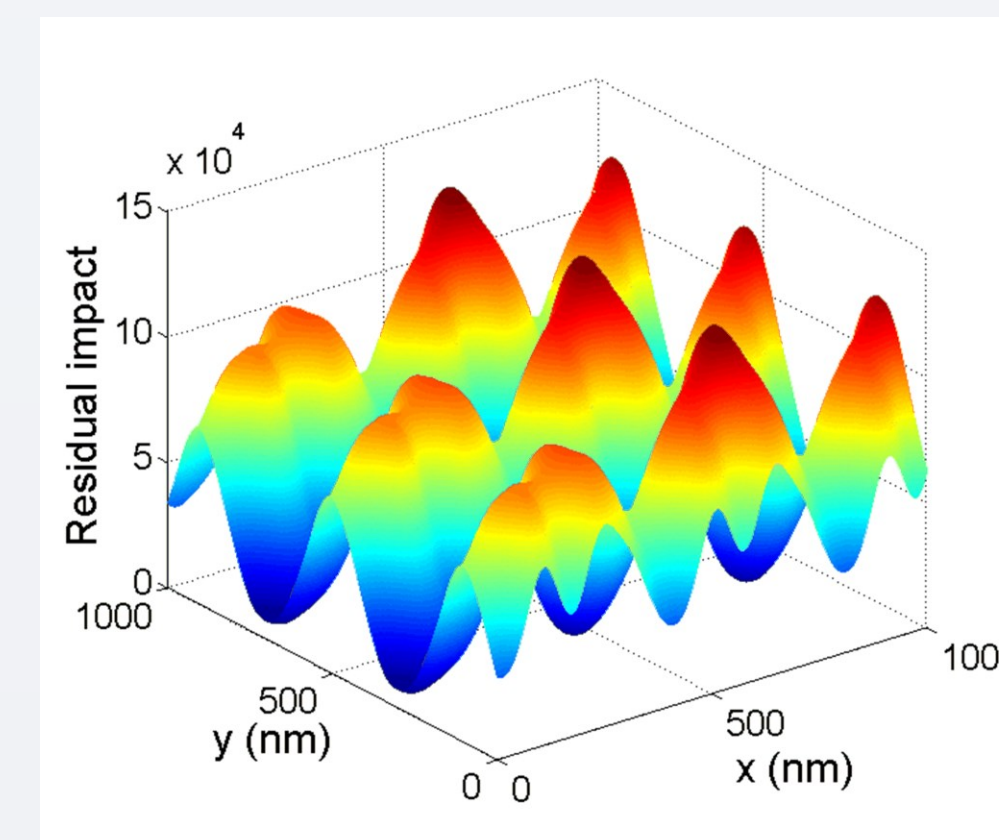


Fig. 5 The residual impact with different shifts (There are 20 defects in the blank).

Defect impact:

$$D(s) = \sum_{i=1}^N \iint_{\text{defect } i} A_{\text{defect}}(i, x, y) \cdot A_{\text{pattern}}(i, s, x, y) dx dy,$$
$$A_{\text{defect}}(i, x, y) = \begin{cases} |h_d(i, x, y)| & \sqrt{(x-x_i)^2 + (y-y_i)^2} \leq FWHM_i \\ 0 & \text{others} \end{cases}$$
$$A_{\text{pattern}}(i, s, x, y) = \begin{cases} 1 & (x, y) \in \text{open region} \\ 0 & \text{others} \end{cases}$$

The merit function of the optimal shift is described as follows:

s : $\text{Max}[T_e(s)]$ after $\text{Max}[N_d(s)]$, when $\text{Min}[D(s)]$,

where $N_d(s)$ is the number of defects covered completely, $T_e(s)$ is the error tolerance(Fig.4), $D(s)$ is the residual impact after shifting.

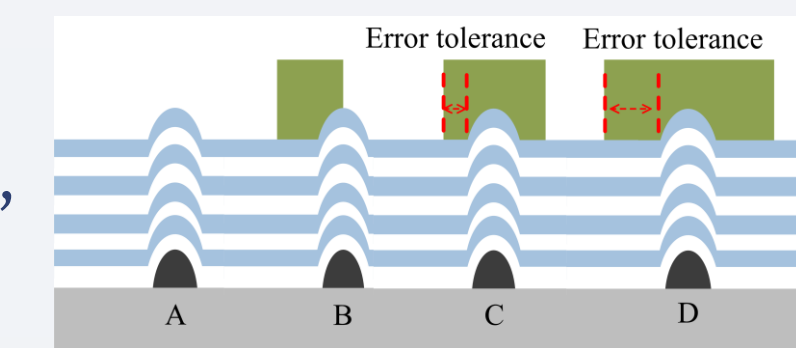


Fig. 4 The error tolerance

The residual impact $D(s)$ with different shifts is shown in Fig. 5. the maximum height and maximum FWHM of defects are 10 nm and 200 nm, respectively. In this case, the residual impact without shifting is 1.067×10^5 , the minimum residual impact after shifting is 6.032×10^3 , and two minimum impact shifts are (17, 294) nm and (17, 694) nm, respectively. The number of uncovered defect is 8.

MAXIMUM NUMBER METHOD

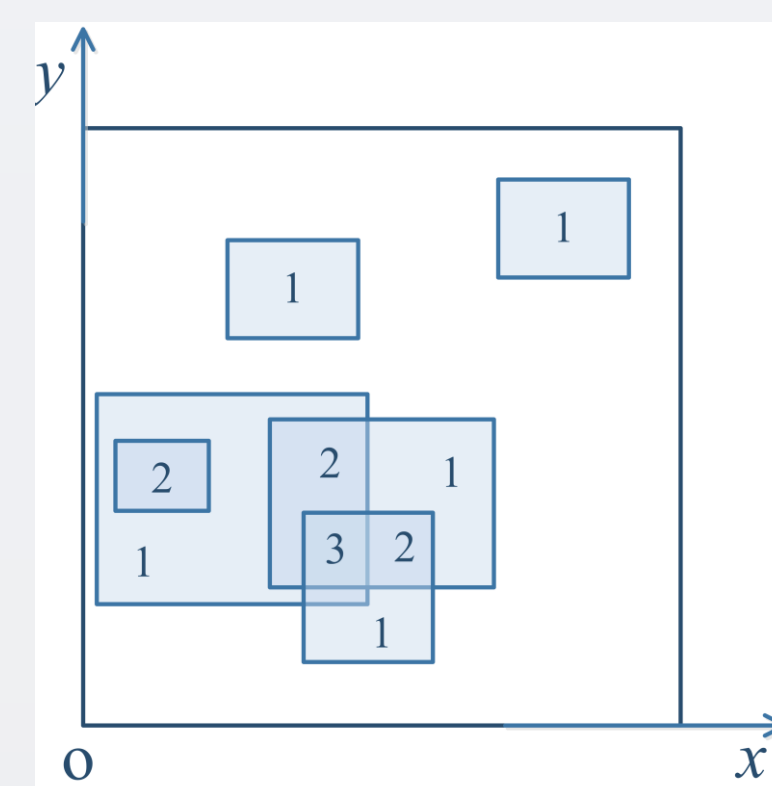


Fig. 6 The definition of overlap of the permitted regions.

The PR of each defect in the blank is determined by

$$PR_{\text{defect } i}(s) = \begin{cases} 1, & \iint_{\text{defect } i} A_{\text{defect}}(i, x, y) \cdot A_{\text{pattern}}(i, s, x, y) dx dy = 0 \\ 0, & \iint_{\text{defect } i} A_{\text{defect}}(i, x, y) \cdot A_{\text{pattern}}(i, s, x, y) dx dy \neq 0 \end{cases}$$

The merit function is described as

s : $\text{Max}[T_e(s)]$ after $\text{Min}[D(s)]$, when $\text{Max}[N_d(s)]$

In Fig. 7, the maximum number of covered defects is 16. The optimal shifts are (70, 317) nm and (70, 717) nm. The residual impact of both is 2.0614×10^4 , which is higher than the result of the minimum impact method. Compared with the minimum impact method, the amount of defects uncovered is reduced; however, the residual impact of some defects is higher. The highest is 1.87×10^4 , which is almost three times that of the residual impact of all defects by the minimum impact method.

COMPARISON OF THE PROPOSED METHODS

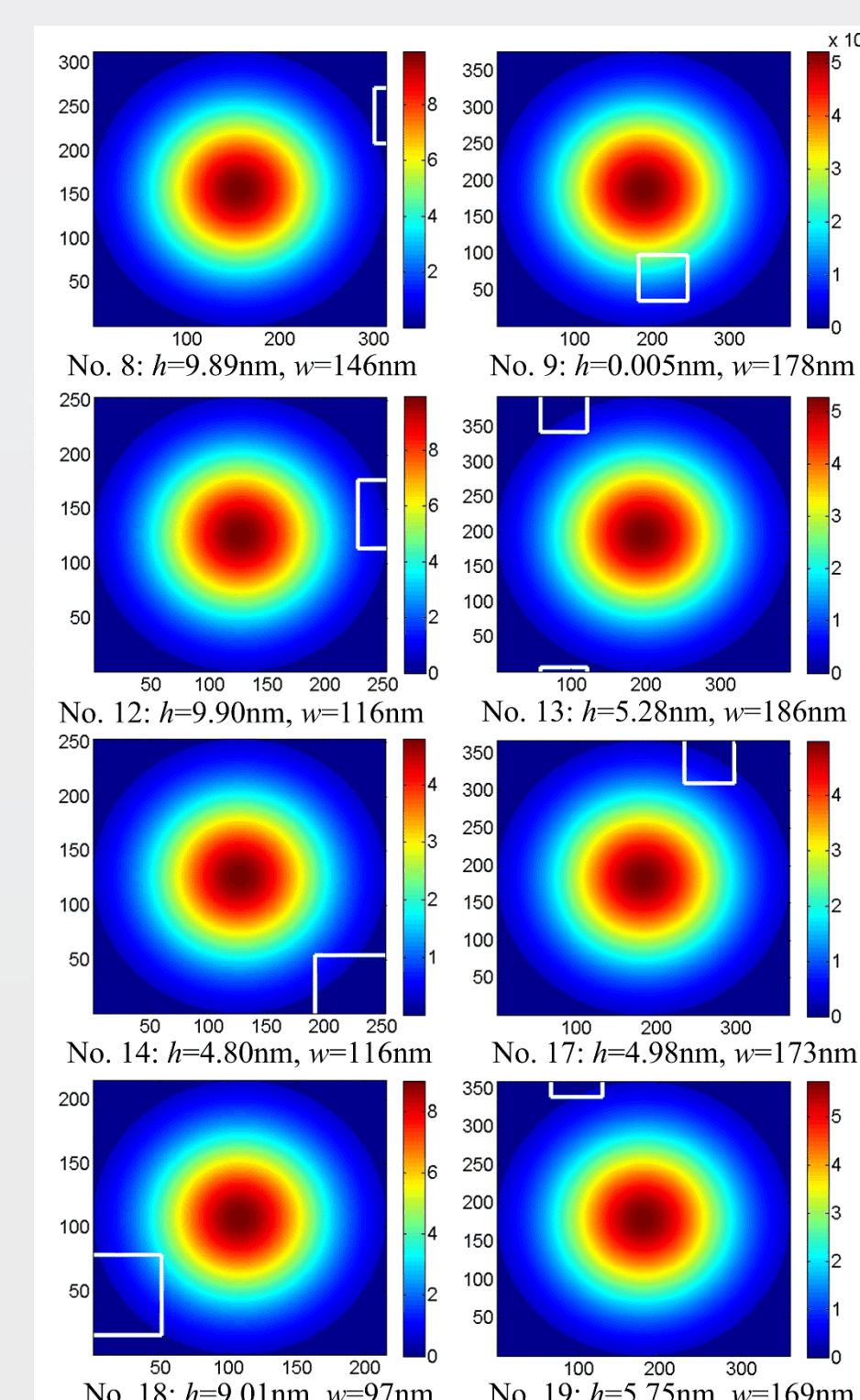


Fig. 8 The residual defects after optimally shifting by the minimum impact method

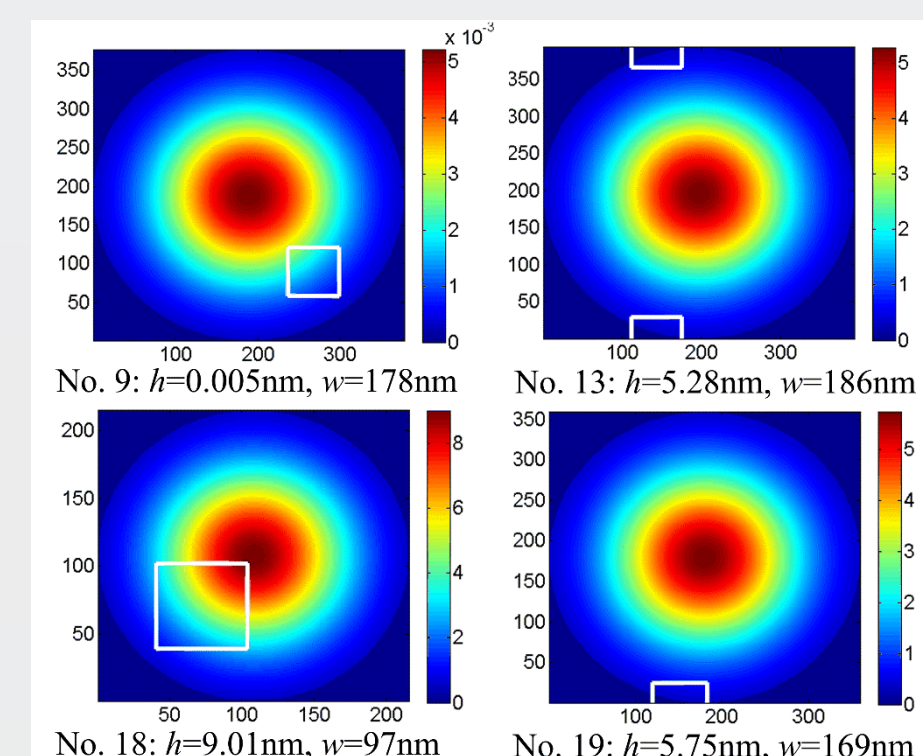


Fig. 9 The residual defects after optimally shifting by the maximum number method (h is the peak height of the defect, w is the FWHM of the defect, the white bordered squares are the open regions, and other part of the defects is under the absorber).

The number of residual defects by the maximum number method is less than that of the minimum impact method (Figs. 8 and 9). However, the residual impact of every defect by the minimum impact method is small, and the residual impact of some defects by the maximum number is very large, especially defect No. 18. Compared with Fig. 8, the open region in the defect region of No. 18 in Fig. 9 is much closer to the peak of the defect. Given the high height of No. 18 defect, its residual impact may not be mitigated or compensated by other methods. Considering the absorber modification method as an example, compensating the residual impact of this defect is unsuccessful.

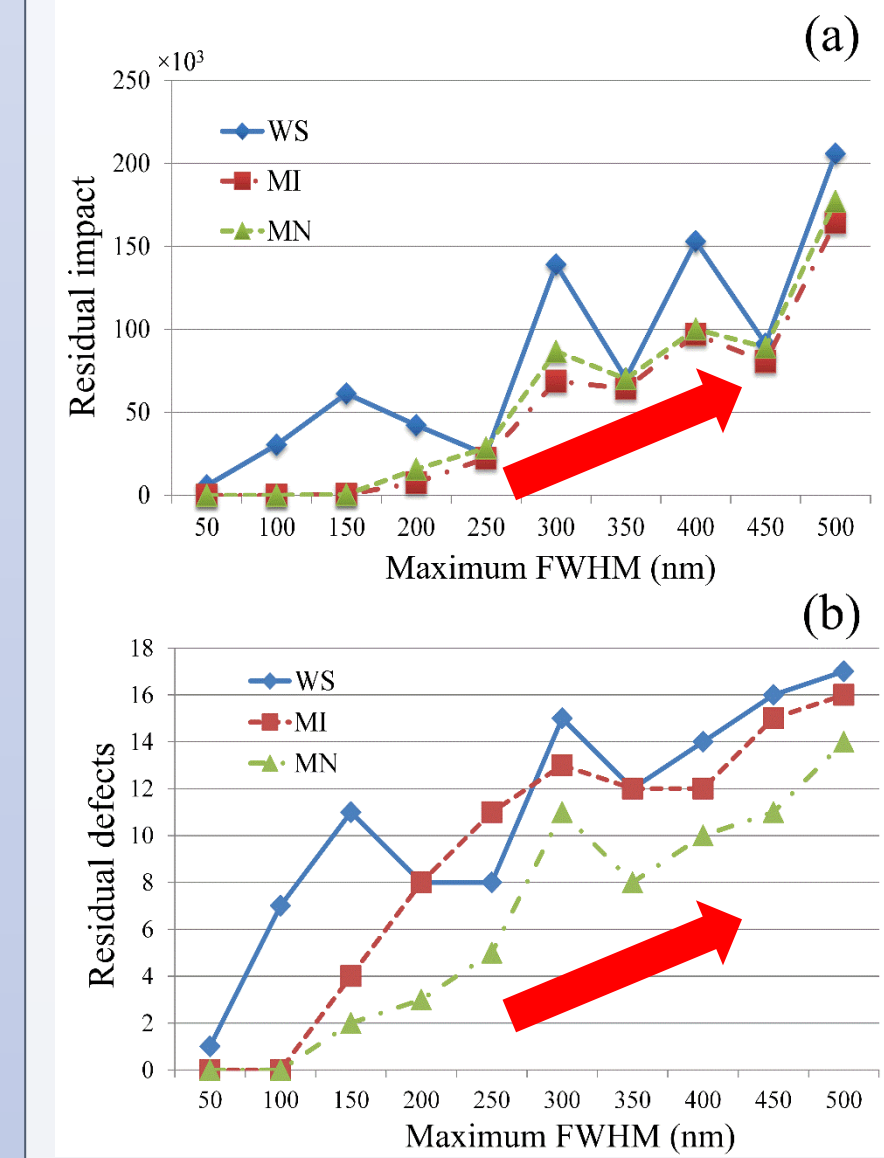


Fig. 10 The residual impact (a) and the residual defects amount (b) as the maximum FWHM increases from 50 nm to 500 nm with an increment of 50 nm.

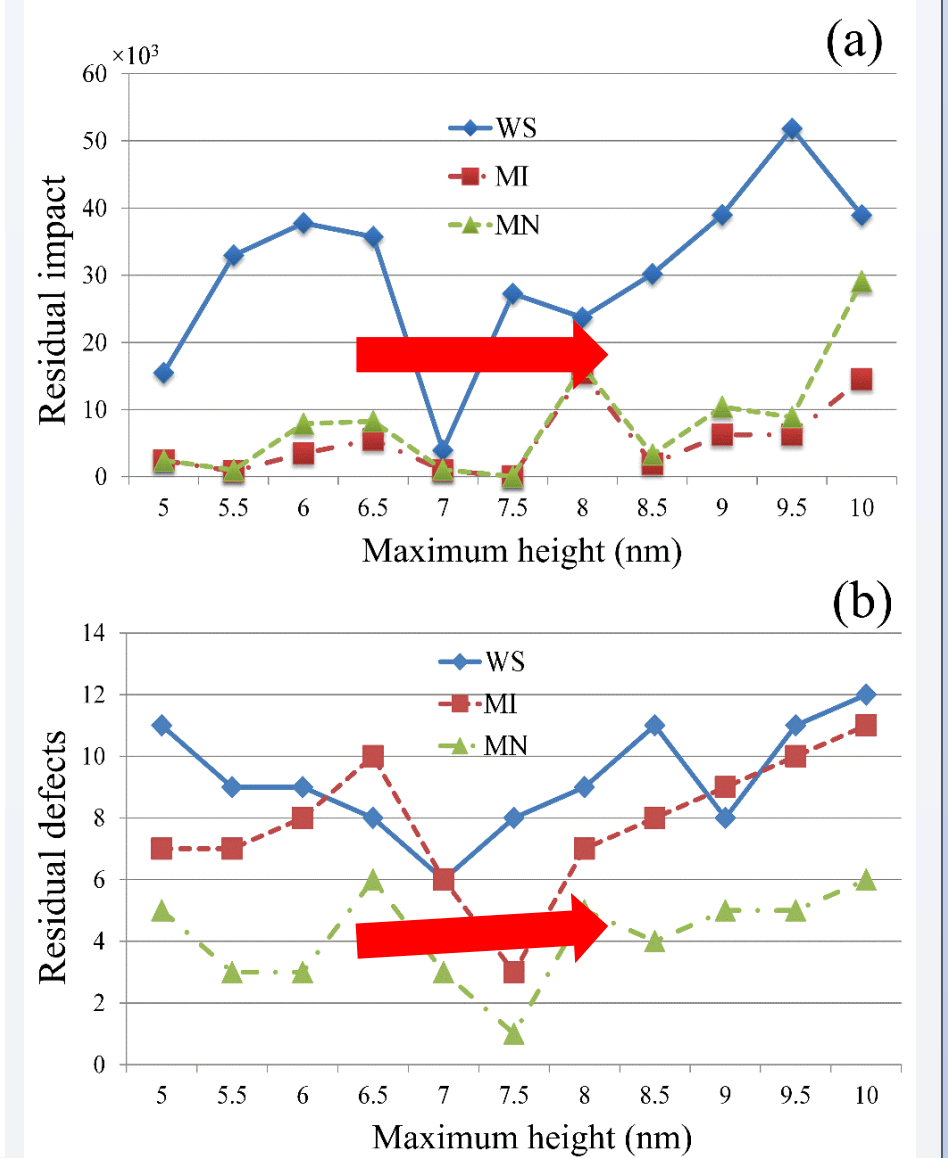


Fig. 11 The residual impact (a) and the residual defects amount (b) as the maximum height increases from 5 nm to 10 nm with an increment of 0.5 nm.

Given the random generation of defect sizes, the increase in the maximum FWHM and maximum height will raise the possibility of generating larger defects. With the increase of the maximum FWHM, both the residual impact and the amount of residual defects generally increase (Fig. 10). However, with the increase of the maximum height in Fig. 11, the increase of the residual impact and the amount of residual defects is not obvious. In pattern shifting, the defect regions determined by FWHM of defects are covered more difficultly as the FWHM increases. Therefore, in view of the mitigation of blank defects, reduction of defects with large FWHM is of higher priority.

CONCLUSIONS

Two methods have been proposed to determine the optimal pattern shift. Compared with the reference without shifting, both the minimum impact method and the maximum number method decrease the impact of defects. Neglecting complexity, and compared with the maximum number method, the minimum impact method is more likely to succeed in the mitigation of defects. The comparisons of those methods with different defect sizes and amounts show that the reduction of defects with large FWHM in the blank is essential for successful defect mitigation.

REFERENCE

- [1] P. Yan, Y. Liu, M. Kamna, G. Zhang, R. Chen, and F. Martinez, Proc. SPIE 8322, 83220Z (2012).
- [2] A. Wagner, M. Burkhardt, A. B. Clay, and J. P. Levin, J. Vac. Sci. Technol. B 30, 051605 (2012).
- [3] C. H. Clifford, T. T. Chan, and A. R. Neureuther, J. Vac. Sci. Technol. B 29, 011022 (2011).
- [4] Elayat, P. Thwaite, and S. Schulze, Proc. SPIE 8522, 85221W (2012).

ACKNOWLEDGEMENT

The authors appreciate the insightful suggestions of Dr. Andreas Erdmann from Fraunhofer IISB. This work was supported by the National Natural Sciences Foundation of China under Grant Nos. 61474129, 61275207, 61205102 and 61405210.

CONTACT INFO

